

# ELECTRICAL DISCHARGES AND BREAKDOWN IN COMPRESSED SULPHUR - HEXAFLUORIDE GAS

**Sayed A. Ward**

Department of Electrical Technology  
Technical College at Dammam  
KingDom of Saudia Arabia

## Abstract

Sulphur hexafluoride (SF<sub>6</sub>) is extensively used as an insulating and arc-quenching medium in gas insulated switchgear (GIS). The gas has a high electric strength, low toxicity, is chemically inert and has good heat transfer properties. These properties allow a reduction in size and enhance the reliability of high voltage (HV) equipment. On the other hand, the dielectric withstand of SF<sub>6</sub> insulated system is extremely sensitive to local in-homogeneity of the electric field, which may result from the presence of defects such as protrusions on electrodes, metallic particles, contaminations, triple junction, etc. These defects cause partial discharges (PD) in SF<sub>6</sub> gas insulated switchgear which in turn are indicative of a possible future breakdown in the system. Therefore, investigations of ways to reduce the effect of such defects are important. The partial discharges and breakdown voltages in compressed SF<sub>6</sub> gas depend on several aspects such as electrode configuration, roughness of electrodes, distribution of electric field, vicinity of insulating supports, moisture, waveshape etc. This paper reviews the mechanisms which lead to breakdown in SF<sub>6</sub> and the phenomenon of partial discharges which occur in compressed SF<sub>6</sub> gas, its causes and the effect of different factors.

## 1. Introduction

In recent years, sulphur hexafluoride (SF<sub>6</sub>) has been of considerable technological interest as an insulating medium in high voltage apparatus because of its superior insulating properties, high dielectric strength at relatively low pressure and its thermal and chemical stability. The high dielectric strength of SF<sub>6</sub> is the result of its being an electronegative gas [1,2], i.e., it tends to trap free electrons and convert them to negative ions.

The excellent insulating properties of SF<sub>6</sub> were utilized in switchgear, and thus gas-insulated switchgear were developed. Compared with conventional air-insulated switchgear, the volume occupied by GIS can be reduced until 2-3% [3]. Thus, they are very advantageous and are in wide use in urban areas where land is hard to acquire [4].

In uniform field, the dielectric strength of pure SF<sub>6</sub> is approximately three times that of nitrogen under the same conditions. However, in non-uniform fields it depends on many factors such as electrode geometry, voltage wave shape, polarity, gas pressure, etc. Although in gas insulated systems a highly non-uniform field would be generally avoided, such divergent fields can occasionally exist due to electrode surface roughness or dust and conducting particles between electrodes [5,6]. As a result of this, breakdown could occur due to local field enhancement which causes partial discharges. Partial discharges are local breakdown phenomena which produce transient current of nanoseconds [7,8]. PD may take place in a

gas, a gas with insulators, and through triple junction [9].

Over the past decade the emphasis in research in the area of PD has been on using it for diagnostic purposes. Significant improvements have been made in the PD detection techniques.

The breakdown voltage of SF<sub>6</sub> gas insulation may be influenced by a large number of parameters such as electrode size and geometry, the material and surface conditions of the electrodes, the properties of the gas, the magnitude and shape and duration of the applied voltage. The effect of these parameters on the breakdown voltages for compressed SF<sub>6</sub> will be reviewed in this paper.

## 2. Partial Discharges in SF<sub>6</sub> Sources and Detection

Partial discharges (PD) are local breakdown phenomena which produce transient currents of nanosecond (10<sup>-9</sup> sec.) duration [7,8]. PD normally involves one of the following combinations of dielectrics [9]:

- Discharges in the gas
- Discharges involving both gas and solid insulation.
- Discharges in a solid component ("electrical treeing" or "cavity discharges").
- Discharges between a system electrode and an electrically floating part.

Typical locations of such defects are shown in Fig. 1.

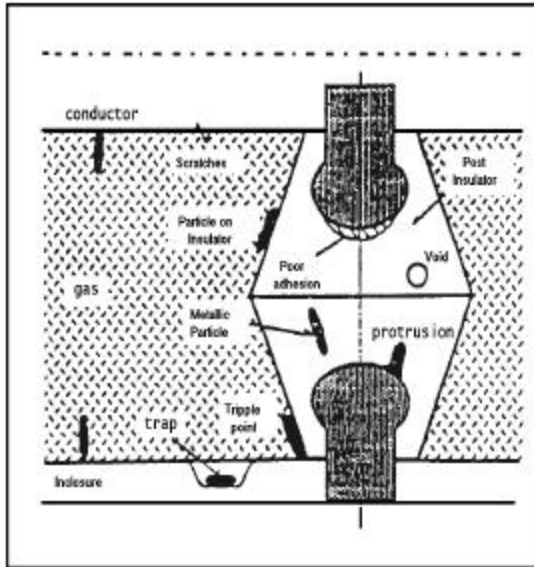


Fig. 1 Possible locations of PD in GIS

PD characteristics may depend on various conditions such as polarity and magnitude of applied voltages, the kind of defects and gas pressure [10,11]. Thus, it is expected that not only the magnitude of PD but PD pulse waveform and hence its frequency component change with these conditions. In other words, the frequency component of PD pulses becomes a key issue to understand the discharge mechanism which should be clarified primarily for highly reliable and accurate diagnosis of insulation performance of power apparatus

## 2.1 Sources of Partial Discharges in SF<sub>6</sub>

In view of the increasing importance of compressed SF<sub>6</sub> as an insulating medium for gas insulated switchgear, it is important to understand the mechanism causing the partial discharges [12]. An understanding of such corona phenomena is also important in the new field of positive-corona electrostatic precipitators. When a high positive voltage is applied to a non-uniform field gap in SF<sub>6</sub> the first corona phenomena to be observed is a sub-nanosecond pulse of current [7,8,12].

Partial discharge in compressed SF<sub>6</sub> gas insulated system can arise from three sources, viz., floating components, free conducting particles, and "treeing" in solid dielectric components [9]. Discharge resulting from the first and last of these sources will, in turn, lead to failure of the switchgear. In the case of a floating component (one not bonded to the conductor or sheath), the discharge magnitude is normally sufficient to decompose SF<sub>6</sub> in quantities, which eventually lead to failure as a result of corrosion. Treeing is a failure process in solid dielectrics which, once initiated will normally proceed to a failure through the bulk of the dielectric.

Aging and failure of insulating systems are initiated by electrical, mechanical, thermal and chemical processes during manufacturing or operation. These create defects reducing locally the dielectric strength of the insulation. At such defects partial discharges can occur, which cause further degradation of the insulation and limit the life time of the equipment. Hence the quality of an electrical insulation system can be characterized by partial discharge measurements which serve to identify type and status of a defect. Typical defects which result from errors in manufacturing, shipping and assembly include losses or electrically floating corona shields, forgotten tools, scratches, and poor electrical contacts are shown in Table (1) [13].

### 2.1.1 Discharges in SF<sub>6</sub> due to contamination and roughness

Conducting particles and surface roughness caused by machining or scratches are known to enhance the local field stress. As a result, the intrinsic breakdown field strength of SF<sub>6</sub> cannot be fully exploited in practical applications. For SF<sub>6</sub> pressures of engineering interest and normal levels of surface roughness, PD inception and breakdown voltages are the same. However PD without breakdown can occur for protrusions above the normal surface roughness. Conducting particles are the most frequent type of imperfection in GIS. Long, thin (wire-like) particles can be lifted in the electric field and occasionally touch an electrode surface [9,14]. The worst-case situation (PD without breakdown) has been investigated experimentally. Two basic types of discharge are observed [13,14], which a quasi-continuous corona like discharge and pulsive discharge which is more common.

Many studies have been devoted to defining a parameter which expresses the harmfulness of partial discharges, and certain international organizations such as the International Electrotechnical Committee (IEC) have recommended certain parameters as being representative of discharge damage. Using the standard IEC 270 PD detection techniques partial discharges can be represented by two quantities;

1. PD magnitude  $Q$  in pi-coulombs and
2. the time of occurrence  $t_i$  in seconds.

The discharge can be represented by the magnitude-phase histogram for AC, and also a three-dimensional histogram should be used for DC. In this representation the phase angle can be substituted by the time between two discharges  $\Delta t$  [17].

**Table I**

**SUMMARY OF POSSIBLE PD-INDUCING DEFECTS IN GIS**

Kind of imperfection	Detectability
Moving particles	The impact of a free conducting particle on the enclosure or on an insulating surface causes an easily detectable acoustic signal. Essentially all types of dangerous particles can be detected. Electrical signals are typically in the range of 20 to 10 pC.
Electrode Protrusions	A corona from a protrusion on an electrode generates a pressure wave in the SF <sub>6</sub> which propagates to the enclosure in which it generates an acoustic signal which can be detected by an acoustic sensor. If the sensor is near the defect, sensitivity is generally better than 2 pC. Electrical detection is also effective.
Fixed Particles on Insulating Surface	Such defects can be detected if they produce corona. Sensitivity is generally in the range of 2 pC.
“Floating Electrodes”	The large partial discharge between a floating electrode and an adjacent electrode produces acoustic pressure waves of much greater energy than corona discharges and is thus easily detected using acoustic sensors. Electrical detection is also very simple as a result of a PD magnitude which ranges up to 1,000,000 pC.
Loose, Non-floating Electrodes	Such a defect, for example a loose corona shield, usually generates PD pulses which are correlated to twice the frequency of the test voltage. Acoustic signals propagate from the defect to the enclosure where they can be detected.
Voids in Solid Insulation, Delaminations	Filled epoxy absorbs high frequency acoustic energy strongly, so that acoustic partial discharge detection is not very effective for detecting voids or delaminations in solid dielectric components. The PD magnitude can range from fC to pC, depending on the size and position of the void. Electrical detection is generally effective for significant defects.

**2.1.2 Discharges from floating components**

A floating component is a conducting element, which is not bonded to the conductor or sheath. Generally, floating components should not be present in GIS unless specifically designed for grading. The most common types of floating components are spacer inserts or corona shields at either the conductor or sheath. A brief analysis of the origin of the phenomenon and the manner in which it can lead to discharge will put the problem in perspective. Floating components normally cause partial discharge with magnitudes in the range of 10<sup>4</sup> to 10<sup>6</sup> pC/pulse with repetition rates of 120 to several thousand discharges

per second, in multiples of 120 Hz [16]. The discharge magnitude resulting from this source is sufficient to decompose SF<sub>6</sub> gas, so that it eventually lead to failure as a result of corrosion.

An electrically floating component (e.g., corona shield) takes a potential, which is determined by the relationship between its capacitance to the conductor vs. that to ground. If as a result of these capacitances and the applied voltage, the component adopts a potential that exceeds its insulation level to the conductor or to ground, the capacitance will discharge. Such discharge tends to be repetitive with a charge transfer in the range of nC to μC (1000 pC to 1,000,000 pC). The discharge pattern is usually

regular, very much like the regular discharge pattern from a cavity as discussed above. However, the PD magnitude is usually larger than for a cavity.

## 2.2 Discharges in SF<sub>6</sub> Under Different Voltages Waveforms.

### AC Voltages

PD characteristics in SF<sub>6</sub> gas depend on various conditions such as polarity, phase angle, magnitude of applied AC voltage. The time-resolved partial discharge measurements in SF<sub>6</sub> gas for a needle-plane electrode arrangement to investigate the frequency component of PD current pulses carried out by M. Hikita and et al [17,18]. The experimental results revealed that PD pulse waveform differed depending on the phase angle when the magnitude of applied voltage and gas pressure were constant. This means that the frequency component of PD pulses differed depending on the polarity and the phase of applied AC voltage.

### DC voltages

It is well known that dielectric spacers supporting conductors in GIS are generally the weakest part of the system. The spacers are directly subjected to various kinds of over-voltages. Furthermore, the dielectric strength of the spacer is affected by local field distortions in the presence of metallic particles or surface charge accumulation. M. Yashima and E. Kuffel [19] measured the flashover voltages and corona discharge current after application of DC voltage for modeled electrode system in SF<sub>6</sub> consisting of a cylindrical spacer with the presence a metallic particle. Surface charge accumulation in the vicinity of the particle under DC stress caused reduction in the flashover voltages of up to 30%.

### Transient Over-voltages

The discharge development in SF<sub>6</sub> gas in case of strong inhomogeneous field conditions is strongly influenced by the applied over-voltage. Important types are Lightning Impulse voltages (LI), Very Fast Transient Over-voltages (VFTO) and composite transient over-voltages (FTO+VFTO), which consists of at least two components with different oscillation frequencies. The discharge developments in case of strong inhomogeneous fields investigate for different transient over-voltages of positive polarity for SF<sub>6</sub> gas pressures up to 0.7 Mpa [20].

The investigation on discharge development was performed in a coaxial electrode configuration with a needle protrusion (length: 7.5mm, tip radius: 0.5mm,

gap distance: 55.5mm), fixed on the surface of the inner grounded conductor under different fast oscillating impulse voltages (2.45 - 12 MHz), the SF<sub>6</sub> gas pressure was in the range from 0.1 Mpa to 0.3 Mpa [21].

A comparison between discharge formation in SF<sub>6</sub> for negative non oscillation lightning impulse and oscillating impulse voltage with an oscillation frequency up to 1 MHz is investigated for a sphere to-sphere configuration with a definite needle protrusion [22], four different voltage shapes (for oscillation) were applied to the test arrangement with impulse amplitudes between 250 and 950 kV depending on gas pressures and impulse shape.

## 2.3 Diagnostic Techniques For Detecting The PD in SF<sub>6</sub> GIS

In order to detect the presence of imperfections/defects, different parameters are measured; namely, electric, magnetic and electromagnetic fields (both inside and outside the GIS), current, voltage, etc. All these parameters are generated by the partial discharge that locally generates small currents with large frequency spectrum that propagate throughout the GIS. They can be classified in three groups according to the frequency range of detection that are conventional partial discharge measurement [23], high Frequency (HF) method, and ultra-high frequency (UHF) method [24]. Depending on the different parameters to be recorded, various kinds of electrical sensors can be used (coupling devices, field sensors, antennas, coils, current probes, etc.) [25].

Recently, different efforts were made to develop methods for using PD as diagnostic tools in SF<sub>6</sub> gas [26,27]. During the latter decade, digital methods in the measurement of PD related electrical quantities have brought new possibilities of PD measurements exploitation both to the evaluation of insulation systems (e.g. to the diagnostic of components) and to the investigation on materials

## 3. Breakdown Mechanisms in SF<sub>6</sub> Gas

Due to the increasing interest in SF<sub>6</sub> as HV insulation, many experimental and theoretical investigations were carried out and reported in the literature to describe the breakdown behavior of SF<sub>6</sub> under various types of experimental conditions and wave shapes of the supply voltage [28-35]. An exact knowledge of the dielectric strength of SF<sub>6</sub> under these conditions is necessary for practical insulation design. Even though various theories proposed to explain the breakdown mechanism in SF<sub>6</sub> have little applications in practical systems, an understanding of these is still essential for the preliminary design of gas

insulated systems. In view of this, the breakdown mechanism is explained on the basis of the various theories proposed along with their limitations.

The situation of BD process for a non-uniform field is much more complex but at least as important. As noted above, SF<sub>6</sub> -insulated apparatus for power engineering use is designed to have little, if any, critical volume (gas stressed above 89 kV/mm. Mpa) at its lightning impulse rating. Therefore if such apparatus fails, almost by definition some defect must have caused an increase of the field over the design value, which almost by definition means an inhomogeneous field condition.

The process by which a small stress enhancement can cause BD of the total gap in SF<sub>6</sub> is as follows. If a free electron occurs in the volume stressed above the critical inception field, that volume would be filled with multiple streamers in a matter of ns. As the field within a streamer is the critical inception field, the streamer can extend only out to a radius from the stress enhancement at which the field falls below critical. At this point, all visible activity stops for a time, during which the (equal numbers of) positive

and negative charges created in the streamers start to separate.

By definition, the field at the boundary of the streamers was at the critical field when visible activity stopped. Thus any charge separation at this boundary will cause the field to go above critical. The increased field caused by the charge separation results in breakdown activity at the streamers bound that culminates in a breakdown from this boundary back to the stress enhancement, but this BD causes a more highly ionized leader, in which the field is only a few kV/cm, i.e, a leader is almost a short circuit and therefore represents an extension of the original stress enhancement into the gas volume. This leader acts as the stress enhancement for the next stage of streamer generation, charge separation, and leader formation. By this process, a small volume stressed over the inception field can cause the entire gap to breakdown through a series of leader steps. The time scale for a leader step is in the range of 100 ns, which means the entire BD process can take over 1µsec, under some conditions. A schematic representation of the BD process with a typical time scale is shown in Fig. 2[2].

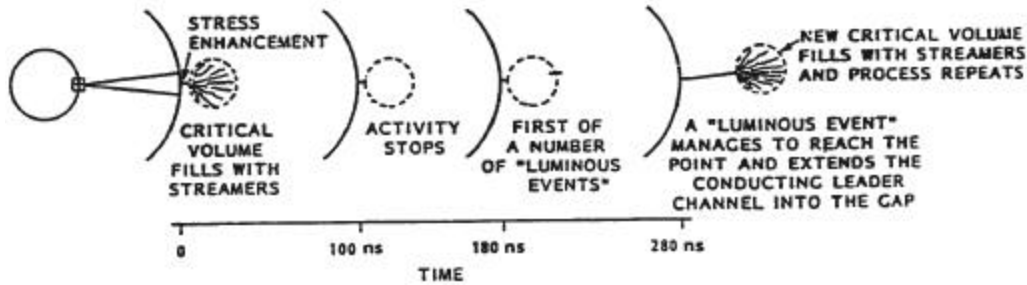


Fig. 2 Streamer -to-leader transition for non-uniform field of SF<sub>6</sub> gas

### 3.1 Streamer Mechanism of BD in SF<sub>6</sub> Gas

The computation of the breakdown voltage for GIS was based on the streamer formation criterion, which assumes a streamer to form when an electron avalanche reaches a critical size. That is,

$$\int_0^x (\alpha - \beta) dx = K_s \quad (1)$$

Where x is the avalanche length, α and β are the coefficient of ionization and attachment; respectively, both being functions of local field E and gas pressure P. There is some controversy over the value of K<sub>s</sub>, the discharge constant. This may vary from one gas to the other; a value of 10.5 is most frequently used in SF<sub>6</sub>, but values up to 18.6 are also used in some analysis

[38]. Considering the available experimental uniform breakdown data, a suitable value for K<sub>s</sub> appears to be 10.5. Equation (1) can be interpreted to mean that breakdown in moderately non-uniform fields or corona in highly non-uniform fields occurs when the total number of electrons in an avalanche attains a certain value.

The performance of SF<sub>6</sub> -insulated equipment is strongly influenced by the presence of high-field sites associated with particulate contamination or surface protrusions, and there is, therefore, considerable interest in the mechanism of non-uniform field breakdown in SF<sub>6</sub>. Studies of the DC and AC breakdown characteristics of such gaps have shown that over a certain pressure range the field at the high-stress electrode is “stabilized” near its corona onset value by the shielding effect of the corona discharge, resulting in a relatively high breakdown voltage. With increasing pressure, the corona stabilization weakens

until, at a critical pressure  $P_c$ , breakdown occurs directly at onset. The effects of factors such as electrode configuration and polarity on corona stabilization and the critical pressure have been reported by a number of authors [28,38,39].

For impulse conditions, the shape of the voltage/pressure characteristic depends on the impulse rise time, with the stabilization peak being more pronounced for the longer rise times when there is sufficient time for space charge shielding to be established. With short rise times, the minimum impulse breakdown level is close to the DC value only up to a certain pressure  $P_1$  less than critical pressure  $P_c$ , and is almost flat in the pressure range  $P_1 - P_c$  [28].

In the above analysis, it was seen that in a non-uniform electric field, the problem of corona formation before the breakdown voltage is reached does assume major significance. Further, Fig.3 shows the relationship of the dielectric strength to the initial corona formation voltage in  $SF_6$  when measured under different pressures with an electrode pair consisting of a sphere of 25mm diameter and a point of tungsten wire having a radius of 0.25mm [34]. The point electrode is, in one instance, of positive polarity and in the other it is of negative polarity. From these figures it can be seen that, in the case of  $SF_6$ , the spread in the voltage between the corona formation and breakdown, under certain pressure condition, is much greater than that which exists for air or nitrogen. Therefore, the ratios co-relating the breakdown relation of  $SF_6$  and air are frequently unsuited for design calculations. Depending on the engineering requirements and the uniformity of the electrical field, the corresponding ratios relating the corona formation voltages may have greater engineering significance. Also, the spark-over voltage in  $SF_6$  for 2.54cm gap between 1.56mm diameter spherical point and a 15.2cm diameter plane under positive DC voltage and AC for  $SF_6$  carried out as shown in Fig. 4. Although different studies for corona stabilization and breakdown voltage for  $SF_6$  under different gap configuration and applied DC and AC voltages was mentioned [34, chapter 2].

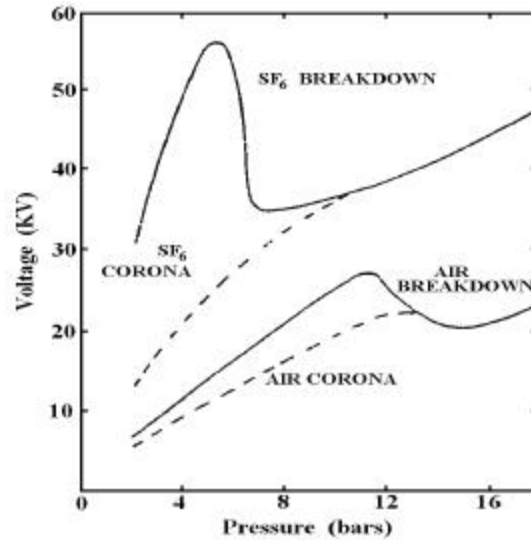


Fig.3 Breakdown and corona inception voltages in  $SF_6$  for positive polarity.

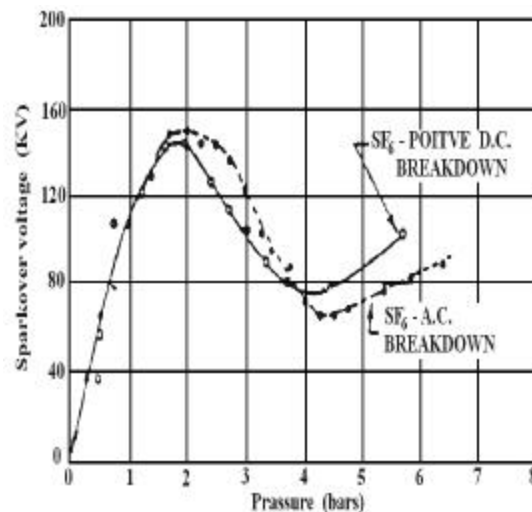


Fig. 4 Spark-over voltage in  $SF_6$  for spherical point-to-plate under DC and AC

### 3.2 Streamer to Leader Transition Criterion in $SF_6$

The phenomena of leader inception and propagation in strongly attaching gases for non-uniform field gaps have been thoroughly studied in the last decade because of their relevance to the design of high voltage gas insulation systems. The streamer-leader transition phenomena are mentioned. There have been many publications covering the breakdown in non-uniform fields gaps [28-33].

A lot of experimental and theoretical work was done to understand the physical process during the discharge under such voltage stress [28-33,40-42]. As a result different breakdown models were developed.

In case of positive LI stress the precursor mechanism describes the streamer-leader transition. Under VFTO stress with a high oscillation frequency and a small damping the high frequency mechanism has to be considered. The corresponding simulation models permit a satisfactory computation of the discharge development, but in each case only for one type of transients [33].

A Similar tool is necessary for the estimation of breakdown levels under composite voltages stress. Streak records demonstrated that in this case the streamer-leader transition is influenced by the precursor and the high frequency mechanism. Based on the physical background of both mechanisms a new universal streamer-leader transition mechanism was found, called energy mechanism [43,44]. The simulation model discussed in the following section allows an accurate calculation of the leader propagation under all steep transients, like LI, VFTO and FTO + VFTO, where no corona stabilization is involved [14]. Buchner [33] describes the leader development in case of strong inhomogeneous fields under LI and FTO stress by the modified precursor model.

### 3.2.1 Modified precursor model for leader BD

The modified precursor model for the calculation of leader propagation under LI and FTO stress of positive polarity has two major characteristics [33];

-A precursor is activated leading to a leader step, if the critical charge  $Q_{crit}$  of the corona is reached.

$$Q_{crit} = 45 \cdot \left( \frac{P}{0.1 \text{ MPa}} \right)^{-1.8} \text{ nc} \quad (2)$$

-After expiration of the delay time  $\tau_p$  between corona formation and the establishment of the leader channel a new leader step can be formed

$$t_p = \frac{3.75 \cdot 10^3 \text{ V} \cdot \text{sec} \cdot \text{Pa}}{P \cdot U} \quad (3)$$

With these equations the leader development can be modeled as follows. The discharge development starts, when the critical field strength  $(E/P)_0 = 89 \text{ kV/mm.Mpa}$  is exceeded. The diameter of the corona  $D_s(t)$  is defined by the different field distribution inside and outside of the streamer corona. Within the corona the field is balanced to  $(E/P)_0$  outside which the geometry of the electrodes determines the field distribution.  $D_s(t)$  can be estimated by calculating the intersection of the internal and external potential curve for each time step. The corresponding capacitance  $C(t)$  is given by accurate field calculations using the Charge Simulation Method. The field distribution

must be calculated for each leader step. The capacitance  $C(t)$  affects a charge  $Q(t)$  of the corona

$$Q(t) = C(t) \cdot [U(t) - (E/P)_0 \cdot P \cdot D_s(t)] \quad (4)$$

with the voltage  $U(t)$  at the tip of the needle reduced by the voltage drop along the corona. In case of subsequent leader steps the voltage drop along the leader is  $E_L(t) \cdot l_L$  with the leader length  $l_L$  considered. In this simulation a time dependent average leader field strength  $E_L(t)$  is used, which describes the effect of leader channel expansion.

After exceeding  $Q_{crit}$  (Eq. 2) the first leader step is triggered. The extension of the streamer corona determines the step length. At the tip of the leader a new discharge is started. In case of a high voltage amplitude the critical charge is reached immediately. After the end of the delay time (Eq. 3) a new streamer region is ionized and the next leader step is created. This development continues until the total gap is bridged[33].

The results for a pressure of 0.3 Mpa are demonstrated for LI [33]. It was noted that the higher pressure effects evidently shorter delay times between the leader steps. This results in an increasing number of steps with a smaller additional length per step. Furthermore only few re-illuminations can be seen compared to 0.1MPa. Fig. 5 shows the calculated leader steps under LI stress for 0.1 Mpa and 0.3 Mpa.

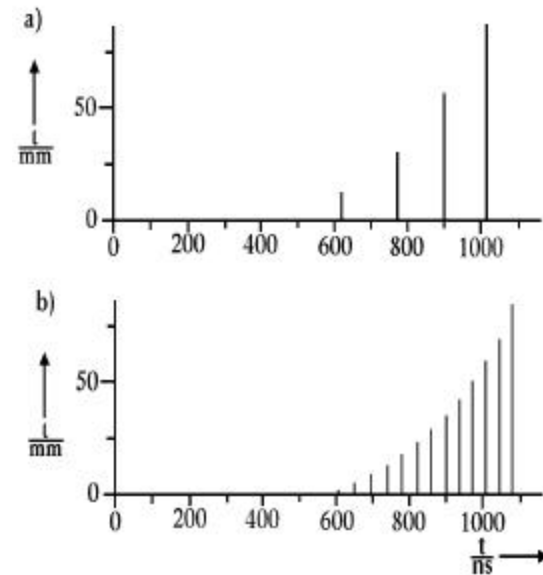


Fig. 5 Calculation of leader propagation a)  $P = 0.1 \text{ MPa}$ , b)  $P = 0.3 \text{ Mpa}$

### 3.2.2 Energy Mechanism for Leader Propagation in $\text{SF}_6$ gas

The model of the energy mechanism allows the calculation of the leader propagation in SF<sub>6</sub> under steep transient voltage stress. In the following the important steps of the calculation are described. Further details are given in reference [44].

The discharge development starts with the formation of a streamer, when the critical value  $(E/P)_0 = 89 \text{ kV/mm.Mpa}$  is exceeded. Considering the different field distribution inside and outside the streamer its time-varying diameter  $D_s(t)$  (Fig. 6 a) can be computed for each time step. Subsequently the capacitance  $C(t)$  of this streamer region towards the grounded plane is determined by accurate field calculations using the Charge Simulation Method. The transient over-voltage  $u^*(t) = u(t) - u_s(t)$  and the capacitance  $C(t)$  cause the displacement current  $i(t)$ ;

$$i(t) = C(t) [du^*(t)/dt] + u^*(t) \cdot [dC(t)/dt] \quad (5)$$

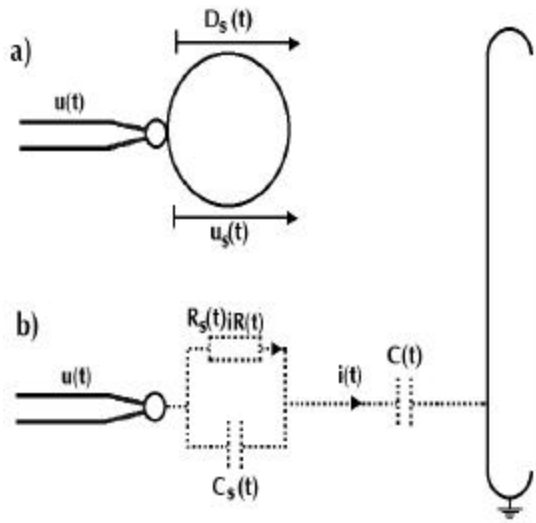


Fig. 6 Modeling of the discharge development in SF<sub>6</sub>

Simplified the essential physical effects in the streamer can be simulated by the network of Fig 6 b. Due to the capacitance  $c_s(t)$  of the streamer itself only the part  $i_R(t)$  of the displacement current  $I(t)$  causes thermal losses resulting in thermal ionization. Considering this network the ionization current  $i_R(t)$  can be computed numerically by solving the differential equation :

$$i_R(t) + \rho_0 \cdot \epsilon_0 \cdot \{d/dt[i_R(t)]\} = i(t) \quad (6)$$

with  $\epsilon_0$  as the dielectric constant. The influence of the pressure-dependent ionization process in the streamer region can be described by the relative ohmic resistance  $\rho_0$  of the streamer. Buchner [43] draw the pressure dependence of the relative ohmic resistance  $\rho_0$  of the streamer. He noticed that, for gas pressures as above 0.3 Mpa they are applied in practice,  $\rho_0$  proves to be constant.

The ionization current  $i_R(t)$  and the voltage drop  $u_s(t)$  along the streamer length pours a significant energy input into the streamer region :

$$W(t) = \int p(t) dt = \int u_s(t) \cdot i_R(t) \cdot dt \quad (7)$$

with  $p(t) > 0$ . The negative parts of  $p(t)$  occur during the re-illumination of the leader. They have no influence on the streamer-leader transition. If  $W(t)$  exceeds the critical energy

$$W_{all}(t) = c_{hit} \cdot \rho_{SF6} \cdot r_{SL}^2 \cdot \pi \cdot D_s(t) \quad (8)$$

(with the critical enthalpy  $c_{hit}$ , the gas density  $\rho_{SF6}$  of SF<sub>6</sub>, the initial leader radius  $r_{ill}$  and the diameter  $D_s(t)$  of the streamer) the gas is sufficiently dissociated and ionized for the leader formation. As a consequence the former streamer region is bridged by a leader channel with a high conductivity. The parameter  $h_{crit}$  is in the range of  $6 \cdot 10 \times 10^6 \text{ J/kg}$ ,  $r_{SL}$  depends on the gas pressure and has values smaller than  $40 \mu\text{m}$  [43].

At the tip of the leader a new streamer is initiated. Thus the next leader steps can be calculated in the same way as described before. The dynamic processes inside the leader channel are considered by using a time-dependent average leader field strength  $E_L(t)$  [42] :

$$E_L(t) = a \cdot [\ln(1 + bPt) / t] \quad (9)$$

The parameter  $a$  and  $b$  describe the dielectric and thermodynamic gas properties of SF<sub>6</sub> with

$$a = 0.3 \text{ V.sec/m}, b = 70 \text{ (Pa.sec)}^{-1} \text{ for LI stress and}$$

$$a = 0.022 \text{ V.sec/m}, b = 220 \text{ (Pa.sec)}^{-1} \text{ for VFTO and composite voltage stress. [43].}$$

Breakdown and volt-time characteristics of non-uniform field gaps in compressed SF<sub>6</sub> gas were studied using a point-to-plane electrode arrangement [45]. Combined voltages, consisting of VFTO and standard LI (STL) voltage superimposed upon DC voltage were applied. The experimental gas pressure ranged from 100 to 500 kPa. The results presented show that the magnitude and the polarity of the direct voltage, as well as the gas pressure influence the corona discharge and the breakdown characteristics. It was found that the breakdown voltages under the VFTO are higher than the corresponding values obtained under standard LI voltages. At the higher gas pressures the volt-time characteristics of VFTO fall below these for SLI.

## 4. Conclusion

Over the past decade the emphasis in research in the area of PD has been on using it for diagnostic



purposes. Significant improvements have been made in the PD detection techniques.

Partial discharge in compressed SF<sub>6</sub> gas insulated system can arise from three sources, viz., floating components, free conducting particles, and “treeing” in solid dielectric components. Discharge resulting from the first and last of these sources will, in turn, lead to failure of the switchgear. In the case of a floating component (one not bonded to the conductor or sheath), the discharge magnitude is normally sufficient to decompose SF<sub>6</sub> in quantities, which eventually lead to failure as a result of corrosion. Treeing is a failure process in solid dielectrics that, once initiated will normally proceed to a failure through the bulk of the dielectric.

A lot of experimental and theoretical work was done to understand the physical process during the discharge under different voltage stress. As a result different breakdown models were developed. In case of positive LI stress the precursor mechanism describes the streamer-leader transition. Under VFTO stress with a high oscillation frequency and a small damping the high frequency mechanism has to be considered. The corresponding simulation models permit a satisfactory computation of the discharge development, but in each case only for one type of transients.

A Similar tool is necessary for the estimation of breakdown levels under composite voltages stress. Streak records demonstrated that in this case the streamer-leader transition is influenced by the precursor and the high frequency mechanism. Based on the physical background of both mechanisms a new universal streamer-leader transition mechanism was found, called energy mechanism.

## 5. References

- [1] S. A. Boggs, “Sulphur hexafluoride : introduction to the material and dielectric”, IEEE Electrical Insulation Magazine, Vol.5-No.5, pp. 18-21, Sept./Oct. 1989.
- [2] S. A. Boggs, “Sulphur hexafluoride - A Complex dielectric”, IEEE Electrical Insulation Magazine, Vol.5-No.6, pp. 16-21, Nov./Dec. 1989.
- [3] S. Yanabu, Y. Murayama, S. Matsumoto, “ SF<sub>6</sub> insulation and its application to HV Equipment”, IEEE Transactions on Electrical Insulation, Vol.26-No.3, pp. 358-366, June 1991.
- [4] K. Nonomura, M. Horikoshi, T. Hasegawa, S. Kimura, N. Itoh, T. Nitta, “Substation design schemes suitable for environmental conditions”, CIGRE Report 23-303, 1990.
- [5] M. M. Morcos, H. Anis, K. D. Srivastava, “ Metallic particle movement, corona, and breakdown in compressed gas insulated transmission line systems”, IEEE Transaction on Industry Applications, Vol.27-No.5, pp. 816-823, Sept./Oct. 1991.
- [6] Sayed A. Ward, “The breakdown voltage for compressed insulated systems with contamination considering the space charge effect”, Conference of IEEE Inter. Symp. on Electrical Insulation, Montreal, pp. 87-70, June 1996.
- [7] E. Kuffel, W. S. Zaengl, High Voltage Engineering Fundamentals, Pergamon Press, Oxford, 1984.
- [8] S. A. Boggs, “ Partial Discharge: overview and signal”, IEEE Electrical Insulation Magazine, Vol.6-No.4, pp. 33, July/August 1990.
- [9] R. Baumgartner, B. Fruth, W. Lonz, K. Pettersson, “ Partial discharge-part IX: PD in gas-insulated substations-fundamental considerations”, IEEE Electrical Insulation Magazine, Vol.7-No.6, pp. 5-13, Nov./Dec. 1991.
- [10] R. J. Van Brunt, M. Misakian, “Mechanism for inception of DC and 60 Hz AC corona in SF<sub>6</sub>”, IEEE Trans. on Electrical Insulation, EI-17-No.2, pp. 106-120, April 1982.
- [11] M. Hikita, T. Kato, H. Okubo, “Partial discharge measurement in SF<sub>6</sub> and Air using phase-resolved pulse - height analysis”, IEEE Trans. on Electrical Insulation, Vol.1, No. 2, pp. 276-283, 1994.
- [12] R. Morrow, “Theory of positive onset corona pulses in SF<sub>6</sub>”, IEEE Trans. On Electrical Insulation, EI-26, No.3, pp. 398-404, 1991.
- [13] R. Baumgartner, B. Fruth, W. Lonz, K. Pettersson, “ Partial discharge- part X: PD in gas-insulated substations-measurement and practical considerations”, IEEE Electrical Insulation Magazine, Vol.8-No.1, pp. 16-27, Jan./Feb. 1992.
- [14] L. Niemeyer, B. Fruth, “Phase resolved partial discharge measurements in particle contaminated SF<sub>6</sub> insulation”, Proc. Int. Conf. on Gas Discharges and Their Applications, Knoxville, paper 82, 1990.
- [15] Peter Morshuis, Gerard Hoogernraad, “Partial discharge diagnostic for DC equipment”, Conf. of IEEE Inter. Symp. on Electrical Insulation, Montreal, pp. 407-410, June 1996.
- [16] S. A. Boggs, “Electromagnetic techniques for fault and partial discharge location in gas insulated cables and substations”, IEEE Trans. on PAS, PAS-101, No.7, pp. 1935-1941, July 1982.
- [17] M. Hikita, T. Kato, H. Okubo, “Partial discharge measurement in SF<sub>6</sub> and Air using phase-resolved pulse - height analysis”, IEEE Trans. on Electrical Insulation, Vol.1, No. 2, pp. 276-283, 1994.
- [18] M. Hikita, A. Suzuki, T. Kato, N. Hayakawa, H. Okubo, “Phase Dependence of partial discharge current pulse waveform and its frequency characteristics in SF<sub>6</sub> gas”, Conference of IEEE Inter. Symp. on EI, Montreal, pp. 103-106, June 1996.
- [19] M. Yashima, E. Kuffel, “ Breakdown characteristics of dielectric spacers with accumulated surface charges in SF<sub>6</sub> under fast oscillating impulse voltages”, 8<sup>th</sup> ISH, Paper 30-04, pp. 267-270, August 1993.

- [20] D. Buchner, "Breakdown of SF<sub>6</sub> insulation in case of inhomogeneous fields under different transient voltage stress", 9<sup>th</sup> ISH, Paper 2268, August 1995.
- [21] B. Heers, K. Moller, "Discharge development in SF<sub>6</sub> under fast oscillating impulse conditions", 8<sup>th</sup> Inter. Symp. on High Voltage Engineering, Yokohama, Japan, Paper 30.03, August, 1993.
- [22] K. Moller, A. Stepken, "Leader formation in SF<sub>6</sub> for oscillating impulse voltages, 6<sup>th</sup> ISH, Paper No. 32.02, 1989.
- [23] T. Kawamura, T. Suzuki, E. Zalma, I. Ohshima, T. Fujimoto, S. Kobayashi, T. Yamagiwa, K. Lbuki, "Development of GIS diagnosis and on-site testing", CIGRE, 1992.
- [24] A. G. Sellars, O. Farish, B. F. Hampton, "Characterising the discharge development due to surface contamination in GIS using the UHF technique", IEE Proc. - Science Measurement Tech., Vol. 141, pp. 118-122, March 1994.
- [25] M. M. Morcos, S. A. Ward, H. Anis, K. D. Srivastava, S. M. Gubanski, "Insulation Integrity of GIS/GITL systems and management of particle contamination", IEEE Electrical Insulation Magazine, pp. 25-37, Sept./Oct. 2000.
- [26] J. M. St-Arnaud, T. K. Bose, M. F. Frechette, "Development of an optical method for the detection of small quantities of contaminants in SF<sub>6</sub>", Conf. of IEEE Inter. Symp. on Electrical Insulation, pp. 114-116, June 1996.
- [27] R. Bozzo, C. Gemme, F. Guastavino, L. Sciutto, "Diagnostic by means of neural networks having inputs derived from the statistical analysis of PD pattern", Conf. of IEEE Inter. Symp. on Electrical Insulation, pp. 389-392, June 1996.
- [28] I. D. Chalmers, O. Farish, A. Gilbert, J. Dupuy, "Leader development in short point-plane gaps in compressed SF<sub>6</sub>", IEE Proc., Vol. 131, Pt. A, No. 3, pp. 159-163, May 1984.
- [29] B. Heers, "Leader propagation in inhomogeneous SF<sub>6</sub> gaps under VFT-stress with critical frequencies", 9<sup>th</sup> Inter. Symp. on High Voltage Engineering, Paper 2267, August 1995.
- [30] K. S. Arunachala Sastry, K. Dwarakanath, B. S. Manjunath, R. Maruti, M. C. Ratra, "Breakdown of SF<sub>6</sub> gas under inhomogeneous fields under impulse voltage of different waveshapes", 6<sup>th</sup> Inter. Symp. on High Voltage Engineering, Paper 32-01, Aug. 1989.
- [31] A. G. Sellars, B. F. Hampton, O. Farish, "Identifying the streamer-leader transition in SF<sub>6</sub> using the UHF Technique", 8<sup>th</sup> Inter. Symp. on High Voltage Engineering, pp. 279-282, Aug. 1993.
- [32] B. H. Lee, T. Kawamura, T. Nishimura, M. Ishii, "Inhomogeneous field breakdown of SF<sub>6</sub> gas under oscillating impulse voltage", 8<sup>th</sup> Inter. Sympos. on High Voltage Engineering, pp. 259-262, Aug. 1993.
- [33] D. Buchner, "The calculation of leader propagation in point/plane gaps under LI and FTO Stress", 8<sup>th</sup> Inter. Symp. on High Voltage Engineering, pp. 255-258, Aug. 1993.
- [34] V. N. Maller, M. S. Naidu, Advances in High Voltage Insulation and Arc Interruption in SF<sub>6</sub> and Vacuum, Ch. 2, Pergamon Press, New York, 1981.
- [35] M. M. Morcos, S. A. Ward, H. Anis, K. D. Srivastava, S. M. Gubanski, "An investigation of particle contamination in uniform and coaxial field", IEEE Electrical Insulation Magazine, Volume 16, Number 5, PP. 25-37, Sept./Oct. 2000.
- [36] H. Anis, K. D. Srivastava, "Particle-initiated breakdown in compressed gas insulation under time-varying voltages", IEEE Trans. on Power Apparatus and Systems, PAS-100, pp. 3694-3702, Aug. 1981.
- [37] N. Antonios, E. Vlastos, "Pressure dependence of DC breakdown voltage and current for SF<sub>6</sub> in the inhomogeneous field", Gaseous Dielectrics III, Pergamon Press, pp. 128-135, 1982.
- [38] Sayed A. Ward, "Assessment of optimum SF<sub>6</sub>-Air, SF<sub>6</sub>-N<sub>2</sub>, SF<sub>6</sub>-CO<sub>2</sub> according to particle contamination sensitivity", Conference of EI and Dielectric Phenomena, Astoria, Texas, USA, PP. 415-418, October 17-21, 1999.
- [39] Y. Qiu, Y. P. Feng, C. Y. Lu, Z. Wu, "Breakdown of SF<sub>6</sub> and some SF<sub>6</sub> mixtures in point-plane gap", 7<sup>th</sup> Inter. Symp. on High Voltage Engineering, Paper 32-09, August 1991.
- [40] Hyeong-Ho Lee, Masanori Hara, "Modification of ion flow field by insulator surface with rod-plane geometry in SF<sub>6</sub>", IEEE Trans. of Electrical Insulation, EI-28, PP. 35-42, Feb. 1993.
- [41] S. M. Mahajan, T. S. Sudarshan, "Measurement of electrical avalanches and optical radiation near solid insulators in high pressure (Up to 0.3 mpa) nitrogen gas", J. Appl. Phys., Vol. 69, pp. 2877-2884, 1991.
- [42] L. Niemeyer, "Leader breakdown in compressed SF<sub>6</sub>: recent concepts and understanding", 6<sup>th</sup> Inter. Conf. on Gas Dielectrics VI, Knoxville, pp. 49-59, 1990.
- [43] D. Buchner, "Breakdown of SF<sub>6</sub> insulation in case of inhomogeneous fields under different transient voltage stress", 9<sup>th</sup> ISH, Paper 2268, August 1995.
- [44] D. Buchner, "Discharge development in SF<sub>6</sub> in case of composite voltage stress", 7<sup>th</sup> Inter. Conf. on Gas Dielectrics VIII, Knoxville, 1994.
- [45] K. Siodla, E. Kuffel, H. Fujinami, "Breakdown of SF<sub>6</sub> in non-uniform field gaps under combined dc fast oscillating impulse and standard lightning impulse voltages", IEEE Trans. on Electrical Insulation, Vol. 28, pp. 253-260, April 1993.